International Journal of Fatigue 178 (2024) 108008

Contents lists available at ScienceDirect

International Journal of Fatigue

journal homepage: www.elsevier.com/locate/ijfatigue

A re-assessment of Ti-685 as a dwell sensitive titanium alloy and a definition for engineering relevant dwell behaviour

M.R. Bache, J. Li *, H.M. Davies

Institute of Structural Materials, Faculty of Science and Engineering, Swansea University, Swansea SA1 8EN, United Kingdom

ARTICLE INFO

Keywords:
Ti-685
Fatigue
Dwell sensitivity
Microstructurally textured regions
Quasi-cleavage facets

ABSTRACT

It is believed that the near-α titanium alloy Ti-685 was the first to demonstrate dwell sensitive fatigue behaviour whilst under engineering service as a gas turbine fan disc material. New fatigue data, micro-textural characterisation and fractography from a recent study which utilised remnant Ti-685 specimens originally manufactured for previous laboratory campaigns based at Swansea dating back to the late 1980s are now reported. In isolation, the present results failed to demonstrate a significant dwell effect in either aligned or basketweave microstructural variants. On this occasion, the limited sensitivity to dwell loading was explained by the combination of heat treatment artifacts and selection of a relatively small test specimen geometry. However, the present data were also reviewed in the context of the wider fatigue database generated by multiple studies over the past fifty years. In combination, stress-life (SN) curves defined the magnitude in applied peak stress necessary to demonstrate a dwell effect in this alloy. Ultimately, this facilitated a fundamental definition of dwell sensitivity that is relevant to the engineering community.

1. Introduction

The phenomenon of "cold dwell fatigue" in titanium alloys was first recognised in the mid-1970s, the consequence of a series of in-service gas turbine fan disc failures [1]. The specific alloy under scrutiny at that time was Ti-685, a near α alloy specifically designed for aerospace applications. Originally intended for high pressure compressor operations, Ti-685 offered relatively superior creep performance when compared to competing alloys. This was the result of thermo-mechanical processing above the β transus designed to induce a coarse grained Widmanstätten or basketweave microstructure. It is presumed that engineering selection was supported by traditional low cycle fatigue assessments of the optimised basketweave variant.

Fractography of the ex-service Ti-685 components invariably indicated crack initiation from sub-surface locations in the thick sections of the disc bore [2]. The focal point of the initiation sites was marked by a crystallographic, quasi-cleavage facet, orientated near perpendicular to the local tensile stress axis. Similar features were later replicated in laboratory specimens. This combination of sub-surface initiation site plus facet orientation conflicts with traditional concepts for early stage fatigue crack initiation which invoke slip induced microscale damage at the material surface [3].

It was also recognised that should the rate of cooling through the beta transus be relatively slow then localised clusters of aligned α plates could form within a general basketweave microstructure. Resulting from thermal gradients and in-homogenous, localised strains, such microstructural variation remains a pertinent feature of thick section forged components including fan discs [4].

Investigations into the fan disc failures conducted in the United Kingdom, deliberately chose the aligned microstructural variant of Ti-685 for detailed mechanical assessment, culminating in a publication by Evans and Gostelow [5]. Crucially, in recognition of typical stress waveforms experienced during service, a clear reduction in fatigue strength was demonstrated in the laboratory when the loading cycle incorporated an extended hold at peak stress (in their case a hold time of 5 min). Together with contemporary laboratory testing based in the United States of America [6] also employing an aligned Ti-685 variant, these publications were amongst the first to report such "dwell debits".

Subsequent research on Ti-685, heat treated to both basketweave and aligned microstructures, supplemented the fatigue database. This continued to demonstrate examples of the sub-surface, orthogonal facet, failure mechanism [7]. However, the volumes of material and number of available test specimens were limited and at that point in time focus was given to the influence of internal hydrogen content [8] and bi-axial stress states (tension–torsion loading). The latter encouraged the use

* Corresponding author.
E-mail address: jing.li@swansea.ac.uk (J. Li).

https://doi.org/10.1016/j.ijfatigue.2023.108008
Received 25 July 2023; Received in revised form 11 October 2023; Accepted 16 October 2023
Available online 17 October 2023

Nomenclature

α	hexagonal close packed alpha phase
β	body centred beta phase
EBSD	electron back scattered diffraction
LCF	low cycle fatigue
MTR	microstructurally textured region
QCF	quasi-cleavage facet
SEM	scanning electron microscopy
SN	stress-life

of a tubular, relatively thin-walled specimen design [7–13]. Consequently, the number of individual specimens available to define stress-life (SN) behaviour under some specific combinations of microstructure and waveform was often restricted.

Different studies on Ti-685 conducted by a range of authors have reported varying degrees of dwell sensitivity in both aligned and basketweave variants [5–13]. Greatest interest has been afforded to the aligned microstructure due to an inferior static and fatigue strength when compared to basketweave material. Collectively, the low cycle fatigue (LCF) data have shown inconsistencies in the measured fatigue strength whether tested under traditional cyclic or dwell waveforms. Reasons for such variation when evaluating dwell sensitive performance will be discussed later.

The current testing campaign employed a batch of solid, plain cylindrical test pieces held over from the Swansea based studies (originally conducted during the mid-eighties to late nineties). The intention was to generate SN curves under load controlled, cyclic and dwell waveforms, avoiding any complexities imposed by the use of tubular specimens and by accumulating an increased population of data points. It was hoped that this would help to establish a threshold level of applied peak stress for aligned and basketweave microstructures above which dwell behaviour was induced. Perhaps of greater importance, these threshold conditions should be considered in terms of fatigue lives, i.e., would any identified dwell sensitivity be of relevance to engineering components or purely offer scientific interest? The present findings, in combination with a review of previous similar studies, raise questions around the selection of test specimen geometry suitable for dwell fatigue assessments in the laboratory and the source of representative materials.

2. Experimental methods

The Ti-685 material (Ti-6Al-5Zr-0.5Mo-0.2Si) employed for the present study was procured back in 1986, the basis for extensive previous research [7–13]. The 30 mm diameter hot rolled bar stock had been solution heat treated and cooled to room temperature to produce either an aligned (slow furnace cool) or basketweave (fast air cool) microstructure, originally described in [7]. After solution heat treatment and aging, the material was machined into mechanical test specimens and since stored in protective sleeving at ambient conditions for approximately thirty years prior to the current investigation. Monotonic strength properties generated for the two variants during the original investigation are listed in Table 1. The applied displacement rate was 1 mm per minute. Although the yield strength data suggest identical properties, definition of this parameter from mechanical stress–strain curves can be prone to experimental and statistical error. The proof stress values, defined from an offset intercept construction technique, are probably more accurate and these demonstrated the superior static strength of the basketweave variant.

Table 1
Monotonic strength data.

	Eng. 0.2 % σ_{proof} [MPa]	Eng. σ_{YS} [MPa]
Basketweave	916	765
Aligned	891	765

In terms of applied fatigue waveforms, to compliment all previous Swansea investigations, the solid plain cylindrical specimens (gauge diameter 6 mm and length 12 mm) were subjected to low cycle fatigue tests under a load controlled 15 cpm “cyclic” or 2 min “dwell” waveform to induce ultimate fracture. The central axis of the solid specimens was coincident with the centre line of the original bar stock. All fatigue tests were performed at room temperature (controlled at 22 °C) with a common stress ratio of R = 0.1. The range of peak stress levels applied to individual specimens was chosen to generate fatigue lives up to a maximum of 10^5 cycles in each microstructure. No run out tests were generated from the present set of experiments.

Optical inspection of the fractured specimens using the naked eye was often sufficient to distinguish the site of fatigue crack initiation as either surface or sub-surface. Higher magnification fractography was performed using a Keyence optical microscope and a Hitachi 3500 SEM. The Keyence system also allowed topographic assessment of the fracture surface, particularly useful for identifying the degree of bulk ductility, extent of circumferential shear lips and relationship between micro-scale quasi-cleavage facets and the immediate surrounding features.

Electron back scattered diffraction (EBSD) measurements employed an Oxford Instruments system supported by Aztec software, with the electron beam set at 20 kV and 0.9 μm step raster. Standard metallographic sections were prepared from material within the gauge sections of multiple post tested specimens (on various planes and well away from the fracture surfaces). An example of near exemplar aligned microstructure is presented in Fig. 1a viewed under electron microscopy. It became evident that an optimum Widmanstätten structure was not present throughout the basketweave variant. Indeed, Fig. 1b shows evidence of aligned colonies within the field of view. EBSD measurements demonstrated that the aligned grains, when found in either host variant, contained extensive colonies of primary α laths, with limited variation in crystallographic orientation within any single grain, Fig. 1c.

EBSD area scans were also taken directly from the fracture surface of selected specimens. Where quasi-cleavage facets were lying orthogonal to the tensile test axis, the specimen was tilted at 70° to the electron beam to enable successful indexing of the underlying hexagonal phase.

3. Results

3.1. LCF response

Fatigue data specific to the two variants are presented in SN graphical form. In each example, separate logarithmic best fit trend lines are superimposed to the cyclic and dwell datasets respectively, described by relevant formulae and reliability values. The aligned variant, Fig. 2, benefits from a greater number of individual test results, which helps better define two distinct regimes of fatigue response under the different waveforms. However, any dwell fatigue debit only becomes evident for specimens tested at the relatively high applied peak stress levels of 850 MPa and above. At this level of stress the alloy is well above static yield and approaching the 0.2 % proof strength measured from this variant.

The number of basketweave specimens available for testing was slightly more limited, Fig. 3. Whereas minimal scatter was noted amongst the cyclic sub-set, a relatively low reliability value for the dwell trend line was evident, reflecting the obvious degree of scatter. Despite the clear difference in the slopes of the cyclic and dwell trend lines superimposed on the data, only the dwell test conducted at the topmost peak stress of 950 MPa displayed an obvious knock down in performance. Again, the stress levels employed at the elevated extreme of the SN curve are comparable to the static proof strength of this variant.

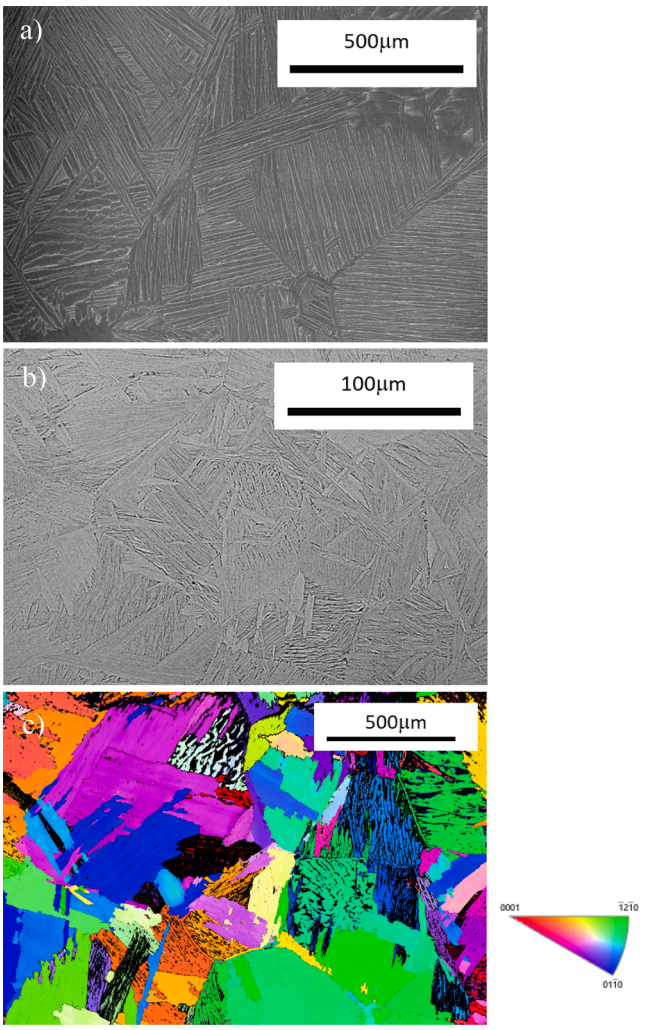

Fig. 1. Typical microstructures: a) aligned (SEM image); b) basketweave (optical image); c) aligned grains characterised via EBSD.

3.2. Fractography

Detailed attention was paid to the precise locations and form of crack initiation in all specimens. Distinct differences were noted according to the relative magnitudes of peak stress applied to the individual specimens but largely independent of the microstructural variant. Typical examples of fatigue fracture are illustrated for the two stress regimes.

Referring back to the fatigue data illustrated in Fig. 2, any aligned variant specimens that illustrated a dwell debit (i.e. applied peak stress levels above 850 MPa) displayed a highly ductile fracture appearance. The cross-section was necked and widespread plastic deformation was evident on the gauge surface (an "orange peel" appearance) to either side of the fracture plane, Fig. 4. In this specific example the gauge diameter was reduced by approximately 10 % on the plane of fracture. The fracture surface exposed the relatively coarse grain nature of the variant, traversing numerous aligned colonies on the macro-scale, Fig. 5, together with microscale ductile tearing, Fig. 6. No obvious crack initiation sites could be discerned in specimens tested at 850 MPa and above. Basketweave specimens tested under relatively high stress conditions also produced ductile fracture surfaces, again without displaying an obvious crack initiation site. Fig. 7 presents the specimen tested at 950 MPa which failed after 108 dwell cycles. Prominent shear lips had formed around the entire gauge periphery.

In contrast, specific sites of fatigue crack initiation were evident in both microstructures when tested under relatively low applied stresses. Fractographic inspections of the entire specimen population confirmed that examples of surface and sub-surface crack initiation were generated irrespective of loading waveform, again in both microstructures. Multiple initiation sites were common, particularly in cases where sub-surface initiation prevailed.

Fig. 8 acts as an exemplar that sub-surface initiation may occur even under the cyclic waveform. This aligned specimen was tested at 800 MPa with failure occurring after 8,562 cycles. A highly reflective, broadly "T" shaped facet had been detected under optical microscopy. Under subsequent SEM view this specific feature appears relatively dark and surrounded by brighter facets containing distinct fan-like, river markings, Fig. 8. Careful manipulation of the fracture surface suggested the surrounding facets to be inclined and this was confirmed using topographic imaging, Fig. 9. This facet was tilted to 70° within the SEM chamber and was subjected to EBSD measurement directly from the fracture surface, confirming that the crystallographic orientation of the α phase microstructure, contained within the bounds of the facet, was predominantly basal, Fig. 10.

The aligned variant specimen tested under the dwell waveform at an equivalent stress level of 800 MPa also illustrated sub-surface initiation, Fig. 11. Again, the relatively flat, quasi-cleavage region representing the site of crack initiation lay approximately orthogonal to the applied tensile axis. At increased magnifications the underlying aligned α lath boundaries could be seen outcropping across the facet surface. EBSD measurements taken directly from the facet indicated a preference for these laths to fracture across their coincident basal planes (highlighted in red). The lack of any indexing from material surrounding the facet suggests the presence of α colonies with inclined basal orientations (i.e., the exposed surfaces are not suitably orientated at 70° to the electron beam to support HCP indexing).

Sub-surface initiation was often suspected in many specimens subjected to the lowest stress conditions, given an absence of distinct, single initiation sites. Instead, a widespread distribution of bright facetted features was noted across the interior regions (each facet lying orthogonal to the tensile axis) when viewed by eye or under low magnification optical microscopy. The example in Fig. 12 was taken from the lowest stress/longest life cyclic test on the basketweave variant (725 MPa, 94,632 cycles). Under SEM inspection facets displayed well defined river marks, Fig. 13a, and when viewed under higher magnification revealed the traces of aligned α laths outcropping at the surface, Fig. 13b.

4. Discussion

The outcomes of the present study will be discussed before considering their wider relevance to the assessment of dwell sensitive behaviour in titanium alloys. A definition of "engineering relevant" dwell fatigue will be proposed and the role of specimen volume/geometry plus material source will be highlighted as key factors when designing laboratory studies intended for characterisation of the phenomenon.

4.1. Present findings

Considering LCF performance, the fundamental SN data presented in Figs. 2 and 3 clearly demonstrate a superior fatigue strength for the basketweave variant over the aligned counterpart. This is consistent with their respective static properties and previous fatigue studies [6–11]. This was irrespective of the fact that the basketweave material contained distributed regions of α lath alignment due to restricted cooling at the centre of the bar stock. The relative difference in fatigue strength, for example measured at a fatigue life of 10^4 cycles, was approximately 40 MPa.

Academia based studies are often restricted in the volume of material available for fatigue testing by cost implications. Where studies are sponsored by engine manufacturers, the extraction of specimens from forged components can be limited due to restrictions imposed by disc geometry. When conducting a cold dwell based LCF assessment, the time

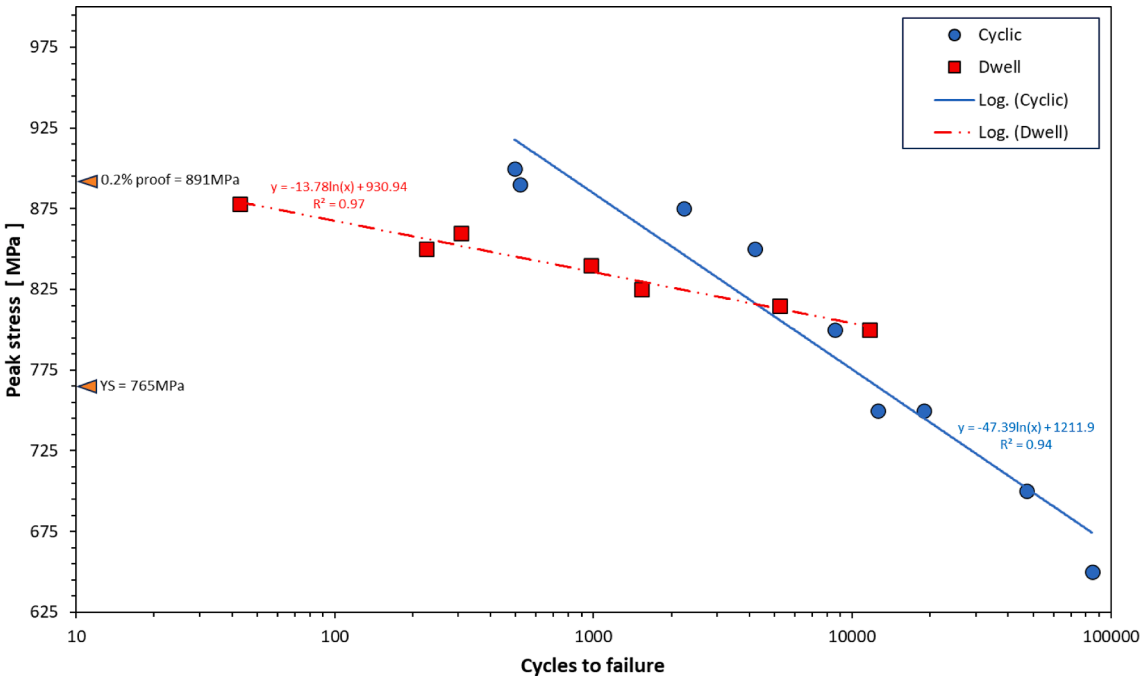

Fig. 2. Fatigue data measured from aligned specimens. (static yield strength and 0.2% proof strength for this variant are indicated).

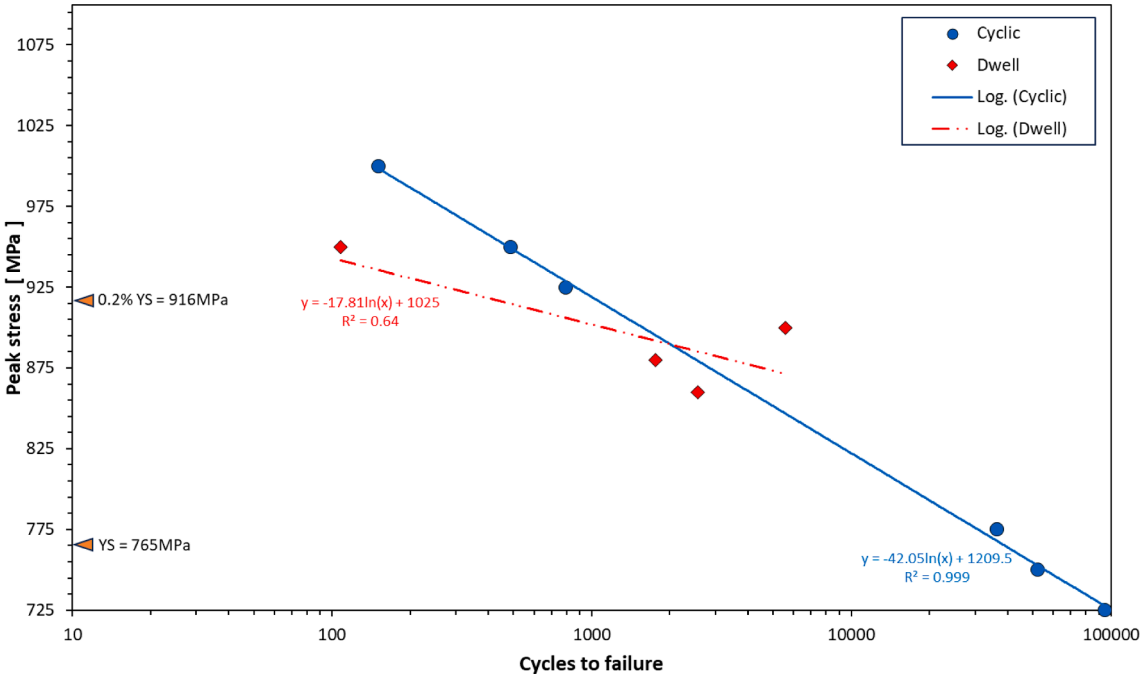

Fig. 3. Fatigue data measured from basketweave specimens. (static yield strength and 0.2% proof strength for this variant are indicated).

Fig. 4. Evidence of plasticity along the external gauge surface of an aligned specimen tested in the high stress regime (dwell waveform, 850 MPa, N_f = 226 cycles).

required to perform dwell tests with a 2 min hold (or greater) at peak stress can also prohibit the number of data points generated to define the dwell SN curve within an acceptable timescale.

Based on a search of open literature, few laboratories have reported fatigue lives for isothermal, room temperature, dwell tests much beyond 20,000 cycles when utilising a dwell time of 2 min or greater. In the case of Ti 685, the longest dwell test reported appears to be that performed by Hall and Eylon [6] to an approximate life of 43,200 cycles (at 5 min hold this single test represents ~150 days of loading). Sinha and co-workers [14] characterised failure in one test that accrued ~45,000 during an assessment of Ti-6246. This laboratory generated what could be the

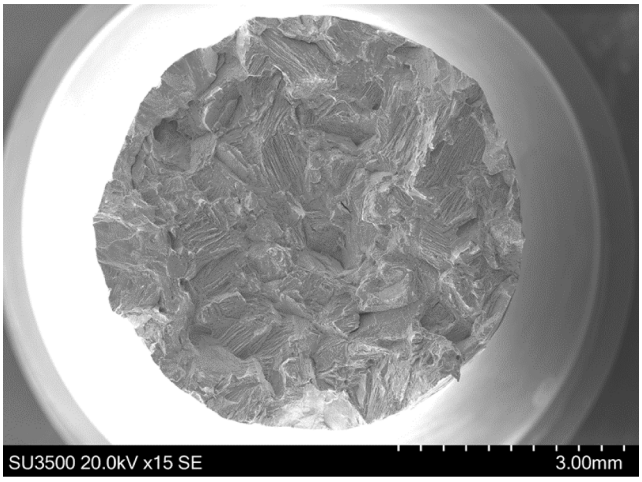

Fig. 5. Aligned variant, fracture surface exposing relatively large grain size and aligned colonies.

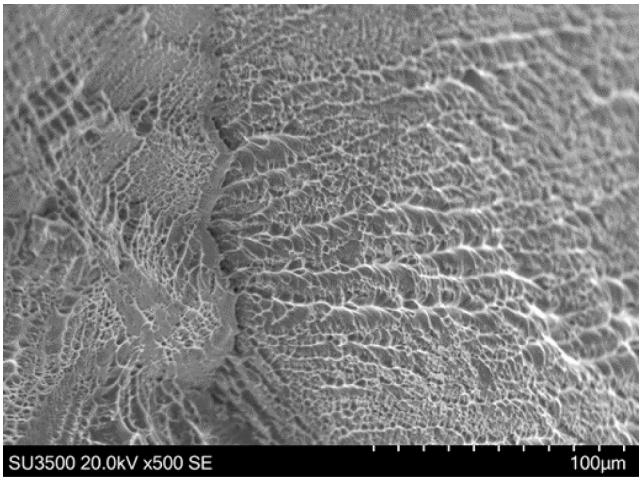

Fig. 6. Aligned variant, fracture surface illustrating region of ductile micro-scale tearing.

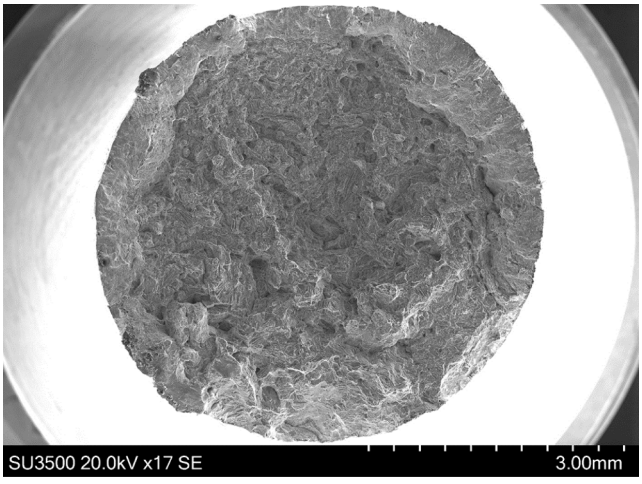

Fig. 7. Basketweave variant, tested under dwell at 950 MPa ($N_f = 108$ cycles).

longest dwell test reported in terms of load reversals, on a Ti 834 specimen which achieved 47,297 cycles (at 2 min hold a single test ran for approximately 67 days [15]). The restrictions imposed by such time/cost issues must be accepted when judging the appropriate number of SN data points required to evaluate dwell sensitive fatigue performance out to very high fatigue lives.

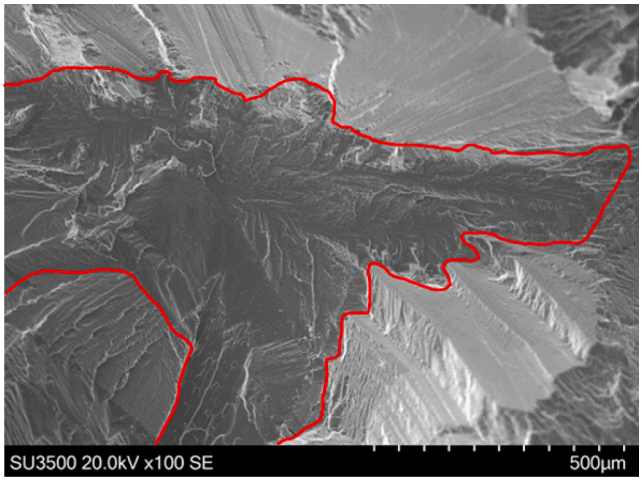

Fig. 8. Aligned variant, orthogonal "T shaped" facet (central dark area bounded by red line) at sub-surface initiation site, fracture under cyclic loading at 800 MPa (8,562 cycles).

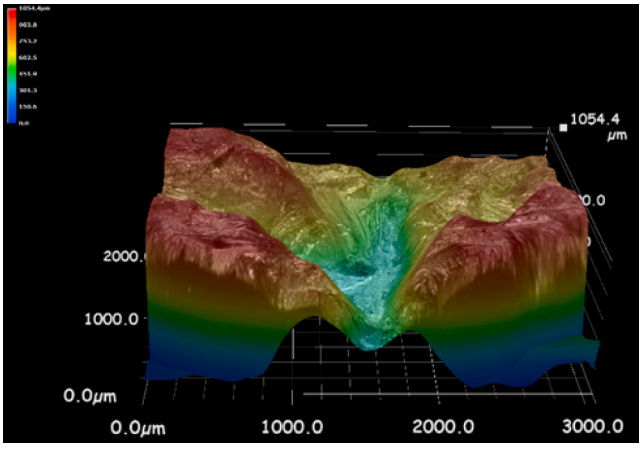

Fig. 9. Topography surrounding the sub-surface facet from Fig. 8.

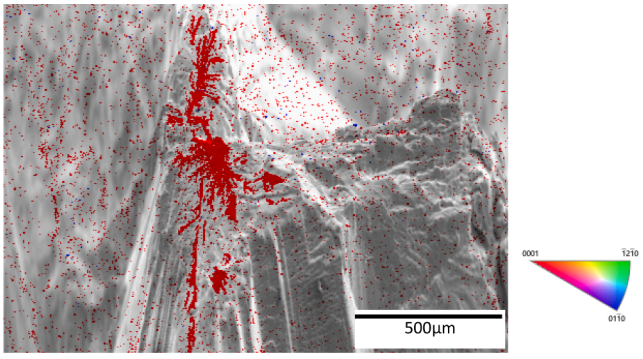

Fig. 10. EBSD measurements taken directly from the facet illustrated in Fig. 8 (fracture surface tilted at 70° to the electron beam).

As a result of this campaign, the increased number of Ti 685 specimens now available to define LCF performance has helped to define more accurate SN curves. Separate logarithmic best fit trend lines were defined for the cyclic and dwell datasets in both variants, with the

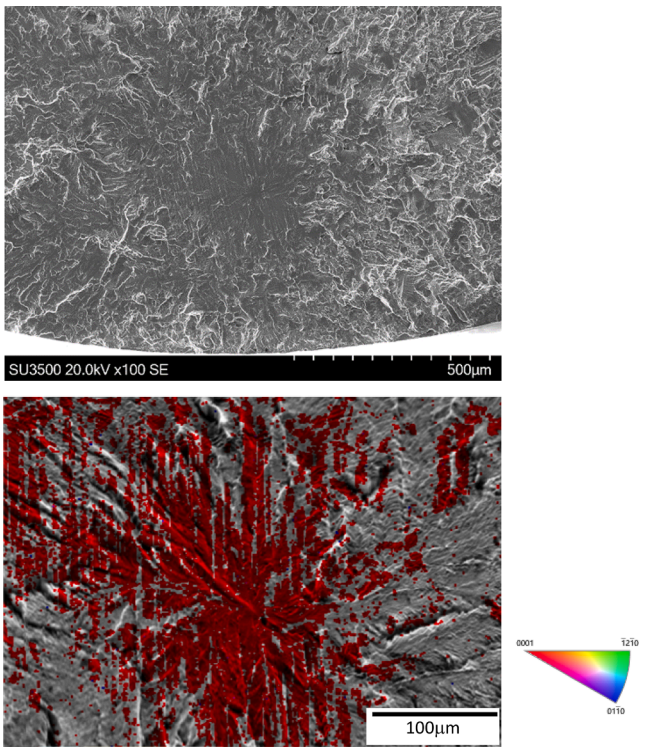

Fig. 11. SEM imaging of sub-surface, orthogonal, quasi-cleavage faceting in an aligned specimen tested at 800 MPa under the dwell waveform. Plan view (top) and inclined to allow direct EBSD measurement from the facet surface (bottom).

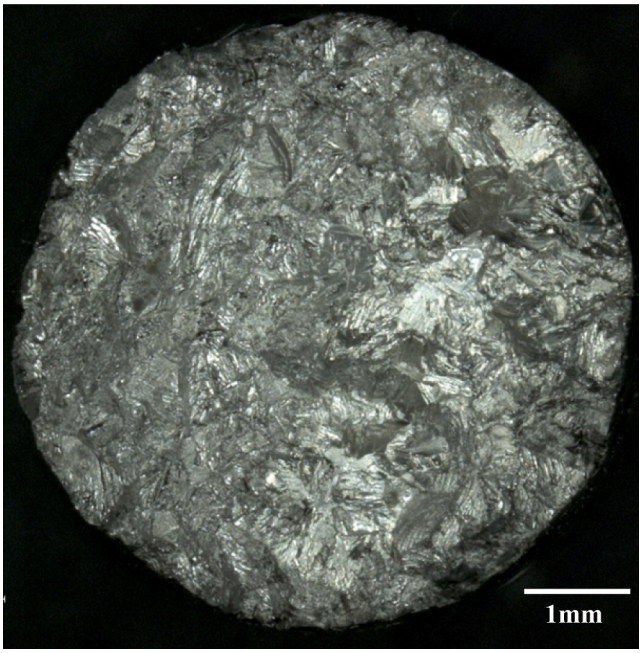

Fig. 12. Basketweave variant, sub-surface distribution of bright facets under optical inspection (725 MPa, 94,632 cycles).

relevant formulae and reliability (r^2) figures superimposed on Figs, 2 and 3. The reliability values are extremely close to unity for three of the individual sub-sets (indicating minimal fatigue scatter), with the exception being the basketweave dwell data with a r^2 value of 0.64, reflecting the greatest degree of experimental scatter amongst this particular variant/waveform combination.

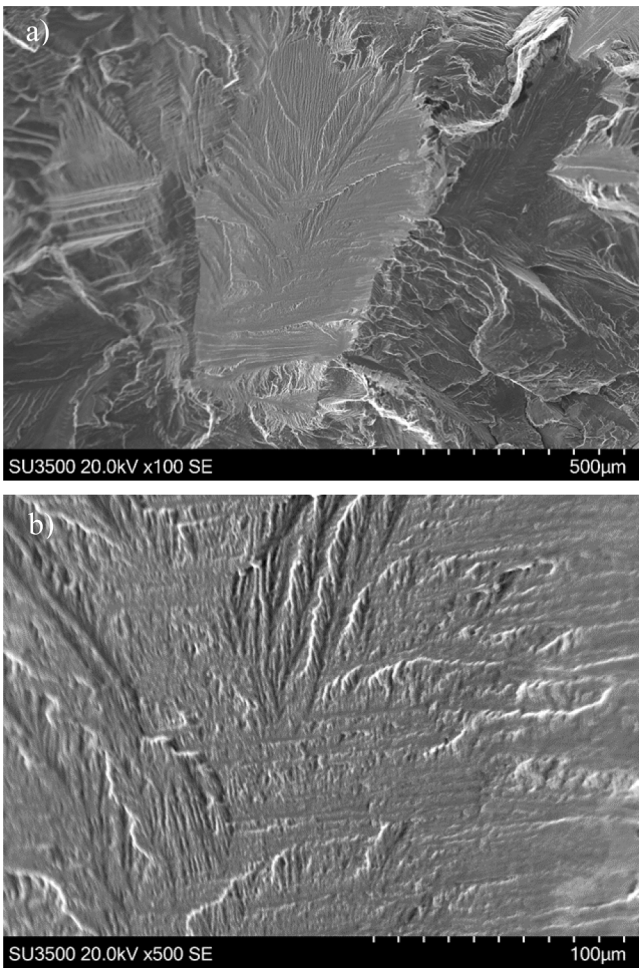

Fig. 13. Basketweave variant, failure under cyclic waveform at 750 MPa (52,221 cycles). a) SEM inspection of a facet illustrating fan like river marks; b) high magnification SEM image showing the exposed traces of aligned α laths.

The trend lines together with direct comparisons between tests performed at identical applied peak stress conditions help to define instances of "dwell debit", i.e., where the dwell test failed under a lower number of stress reversals compared to the equivalent cyclic test. A marked dwell debit was only displayed in the basketweave variant under the highest-most peak stress test condition of 950 MPa, Fig. 3. This specimen survived as few as 108 cycles. It is interesting to note that an attempt to run a test at 50 MPa above this level actually failed during the first loading cycle. This emphasises the very high levels of applied stress necessary to induce a dwell effect in this variant during the present study. These stress levels certainly exceed the proof strength of the variant and time dependent, room temperature "cold creep" would be prevalent during the individual dwell periods at such conditions [16]. Engineering components would not be designed to operate under such high stress environments.

On this occasion, the aligned variant possibly presents a more compelling case for dwell sensitivity, Fig. 2. When compared to the best fit trend line drawn through the cyclic data, three specimens tested at 850 MPa and above all failed at lives approaching one order of magnitude lower. However, the applied stresses necessary to induce this dwell debit were once again substantial relative to static properties.

Fig. 14 combines the best fit trends measured from aligned and basketweave specimens to visualise and emphasise the effect of microstructure on fatigue strength. The SN space between the extremes of aligned and basketweave performance have been shaded for the dwell and cyclic conditions (in red and blue) respectively. It appears

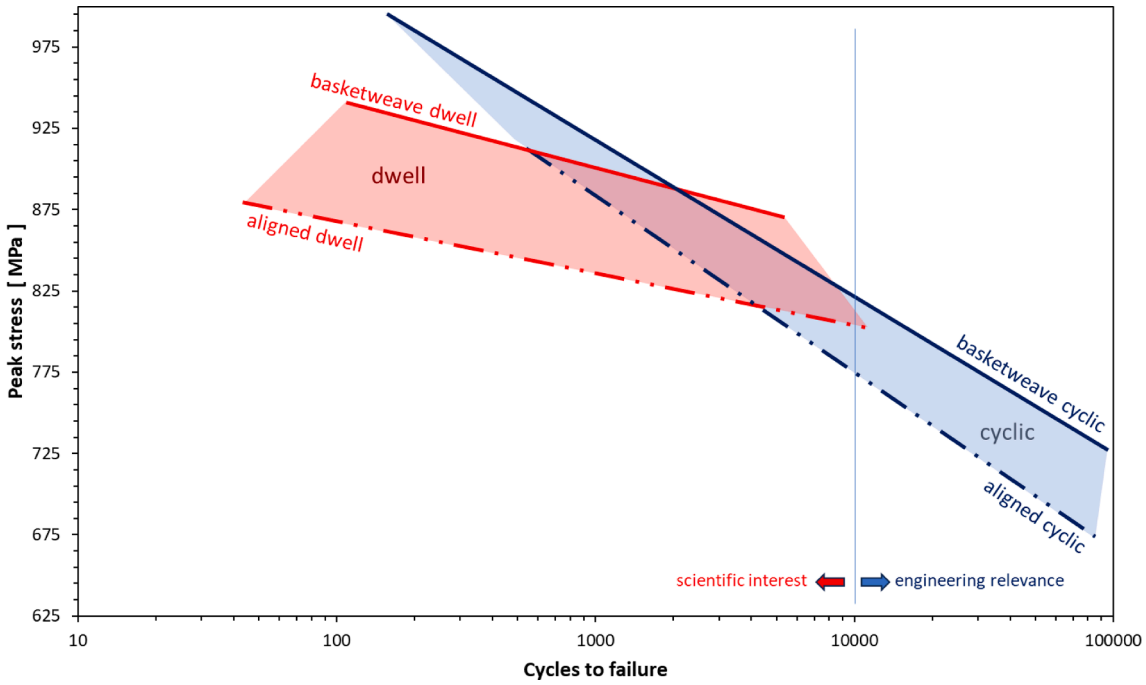

Fig. 14. Relative LCF performance due to extremes of aligned and basketweave microstructures.

reasonable to assume that fatigue performance for intermediate microstructures falling within these optimised extremes (i.e., increasing volume fraction of alignment within a general Widmanstätten microstructure) would be matched by a progressive change in fatigue strength between these bounds. It also becomes apparent that due to the low slope in the SN curve defining dwell behaviour, the potential for high scatter in fatigue life to failure between multiple or repeat tests at any specific applied stress condition is significant.

It is certainly the case that for the fatigue life regime greater than 10^4 cycles, where greatest engineering interests would lie, the present evaluation employing hot rolled bar stock material has failed to characterise any degree of dwell sensitivity in either microstructural variant. Indeed, it could be argued that any sensitivity defined by the present study constitutes "scientific interest" only. Future assessments may wish to adopt the proposed definition of "engineering relevant dwell sensitivity", i.e. only deem an alloy to be prone to dwell if life debits are measured for cyclic lives of 10^4 cycles or greater.

Both microstructural variants demonstrated highly ductile, shear dominated failures in specimens tested at the relatively high stress / short life test conditions - irrespective of waveform, Figs. 4 to 7. Despite the limited number of slip systems available in α phase titanium crystals [17Williams] it was apparent from simple optical inspections that many grains within these specimens had exceeded a critical value of resolved shear stress. On this occasion, bulk cyclic strain accumulation was not monitored from the individual specimens. However, previous studies from this laboratory have reported such data [e.g. 7,9,10,16]] and it has been demonstrated that:

- aligned specimens accumulate greater strain than basketweave (when subjected to an identical applied peak stress),
- failure strains under dwell loading exceed those under cyclic waveforms, and
- the magnitudes of strain accumulated at failure increase with applied stress levels.

Based upon machine stroke data available from the current matrix of tests, we are confident that similar bulk plastic behaviour was again evident. At relatively high magnitudes of applied stress, bulk plasticity or "cold creep", appears to dominate fracture behaviour and specimens ultimately fail through a ductile shear mechanism, revealing no distinct site of crack initiation.

Quasi-cleavage facets marking the epicentre of crack initiation events were most obvious on the fracture surfaces of specimens tested at relatively low applied stress levels. These low stress tests accumulate relatively less bulk cyclic strain irrespective of waveform or microstructure. Examples of facets orientated orthogonal to the tensile stress axis were common in the aligned variant. Examples are illustrated in Figs. 8 and 11, notably generated under cyclic and dwell waveforms respectively. EBSD measurements illustrated that such facets traversed colonies of aligned α laths with coincident basal planes, Figs. 10 and 11. Neighbouring colonies or grains that immediately surround the facet were apparently orientated with their basal planes inclined to the tensile axis, therefore more favourably orientated for slip. Hence, the microstructure and associated textures of the two examples of quasi-cleavage faceting presented here were consistent with the modified Stroh "strong–weak" neighbour model for facet formation [17]. Modified by Evans and Bache [9] the model invokes differences in the time dependent flow properties of neighbouring grains.

As the peak stress levels applied to individual specimens decreases (i.e. towards the lower end of the SN curves), so does the number of grains favourably orientated to exceed the critical resolved shear stress on inclined basal planes. Subsequently, the probability that juxtaposed "weak-strong" grain pairings exist is also reduced. Together with the absence of general plasticity in the surrounding material, quasi-cleavage facet initiated failures become more apparent under low stresses.

Evidence from numerous alloys and varying thermo-mechanical products have since demonstrated that MTRs of common orientation can also induce significant dwell fatigue failures with clusters of facets distributed over relatively large areas [15,18,19]. Under the current scenario, it is argued that colonies of aligned α laths, with each lath having the same crystallographic orientation, essentially constitute a form of MTR. In this fashion, the colonies can act as a single effective structural unit of considerable size (over 500 μm in cross section). Notably, aligned colonies existing within the basketweave variant often appeared to act as crack initiation sites, Figs. 12 and 13. In the context of the Evans-Bache faceting model, any aligned regions will offer an

increased slip band length, encouraging dislocation pile ups at the neighbouring grain boundary and increasing the magnitudes of shear and tensile stress locally redistributed onto the strong grain.

4.2. Specimen geometry and volume

Selecting the optimum ratio between specimen size and effective structural units appears to be a critical concern during the design of experiments intended to characterise dwell sensitivity. At first sight, the resistance to dwell sensitivity currently demonstrated in the basketweave variant appears inconsistent with previous findings [7–11]. One reason behind this could be the scale of the solid specimen currently employed. The inherently large grain size of Ti-685, whether processed into an aligned or basketweave microstructure, has been demonstrated, Fig. 1. The volume of critically stressed material within the gauge of the 6 mm diameter solid specimens was 340 mm^3. If accepted that dwell behaviour is intimately related to specific crystallographic entities offering "weak links" (i.e., intimate neighbours of strong and weak grains or colonies) the probability of sampling such combinations is reduced when employing a small specimen design.

It is interesting, therefore, to compare the current data to a very limited dataset reported in [9], representing cyclic and dwell tests performed on the same aligned material using a larger, solid specimen geometry (9 mm diameter, gauge volume 1590 mm^3). Referring to Fig. 15, the 9 mm solid specimen data correlate extremely well under the cyclic waveform. However, under dwell, although the highest stress test conducted at 850 MPa compares well with the present dwell trend, a slightly weaker response was indicated at the relatively low stress regime. The minor extent of the dwell debit measured at 750 MPa (x2) probably influenced the conclusion stated in [12] that the aligned variant was insensitive to dwell. This also illustrates that some interpretations of previous Ti-685 studies relied on a minimal number of fatigue data points in some instances. In any case, the 9 mm database demonstrates a dwell debit in the regime that encroaches that of engineering significance.

Finally, when considering specimen geometry, the data plotted in Fig. 16, again taken from reference [9], confirms an overall, relatively weaker response measured from tubular specimens (with 6 mm inner and 9 mm outer diameter) in the aligned variant, when subjected to uniaxial tensile fatigue cycles and compared to the present 6 mm solid database. Notably, referring back to Fig. 1, the tubular specimens could be sampling a very small number of grains within the 1.5 mm wall section.

4.3. Material source

It has been argued that the present investigation failed to detect a dwell effect in Ti-685 of engineering relevance. This is in sharp contrast with early assessments published by [5,6] in the immediate aftermath of the reported Ti-685 fan disc failures. Data from aligned [5] or "large colony" [6] specimens are superimposed on the present aligned best fit trend lines in Fig. 17. Note the data points from [5,6] have been digitised from the original publications. Three points were deliberately ignored from [5] to omit any run out tests or where the same specimen had been tested at two different stress conditions. In the case of [6], one dwell test and one cyclic test were ignored, relating to failures deemed to initiate from specific "forging defects" (porosity). Notably, all data represented on Fig. 17 were generated from similar sized solid, plain specimens (i.e. diameters ranging from 6.0 to 6.5 mm).

Eylon and Hall [6] measured the greatest difference between cyclic and dwell waveforms. Employing a five minute dwell period, comparing tests at a common applied peak stress of 830 MPa, an unprecedented dwell debit of approximately two orders of magnitude was noted. Their cyclic data appear to demonstrate a distinctly strong fatigue response, but this may be explained in part by the fact that their experiments were performed at an elevated mean stress condition (R = 0.3) and the data are presented here on a peak stress basis. In comparison the dwell debit illustrated by Evans and Gostelow, although considerable, was less (a factor of approximately 16 was quoted).

However, vital differences in the source materials are noted across the combined studies illustrated by Fig. 17. Eylon and Hall extracted specimens from an actual fan disc forging, deliberately sampling regions containing as forged, aligned microstructure. In contrast, Evans and Gostelow employed small section, rectilinear forged bar subject to a low degree of hot work [20] which was subsequently solution heat treated under vacuum to provide the aligned variant. Unfortunately, prior to the

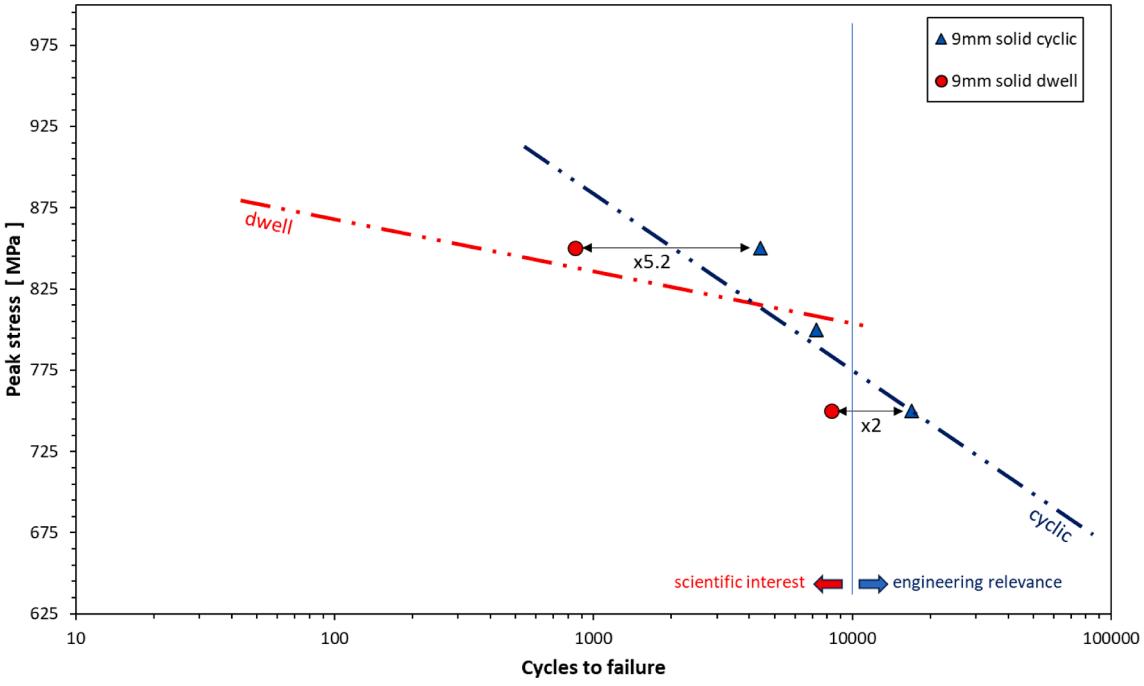

Fig. 15. Effects on LCF performance due to solid specimen size (data points from [9]).

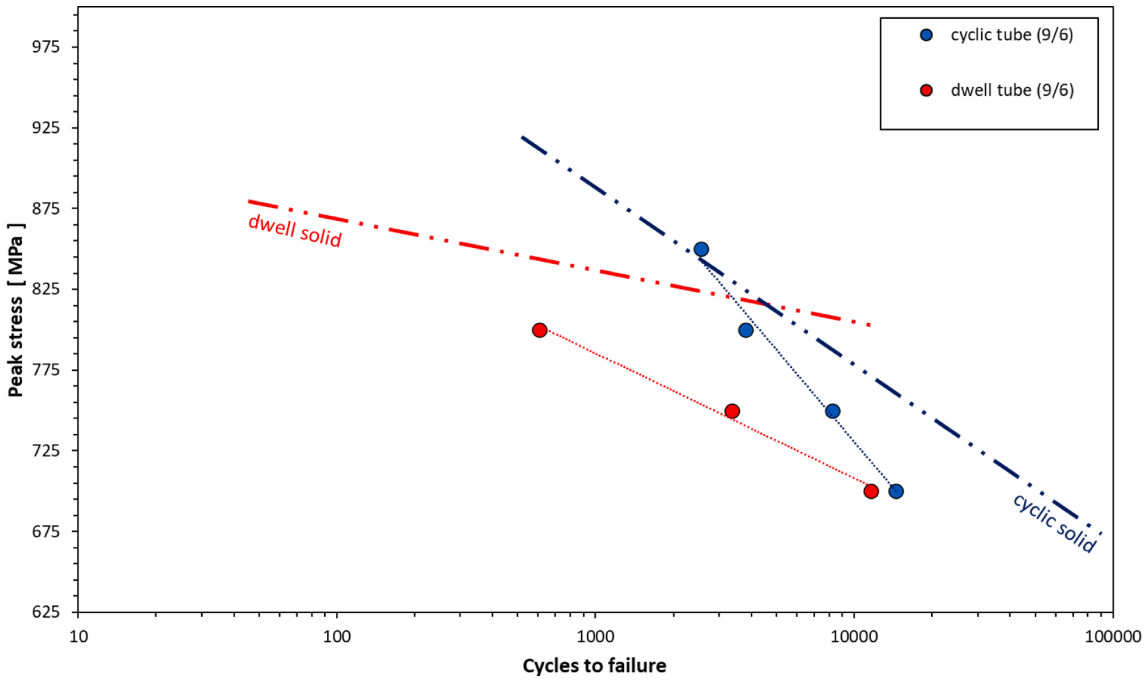

Fig. 16. Effect on LCF performance due to specimen geometry (data points from [9]).

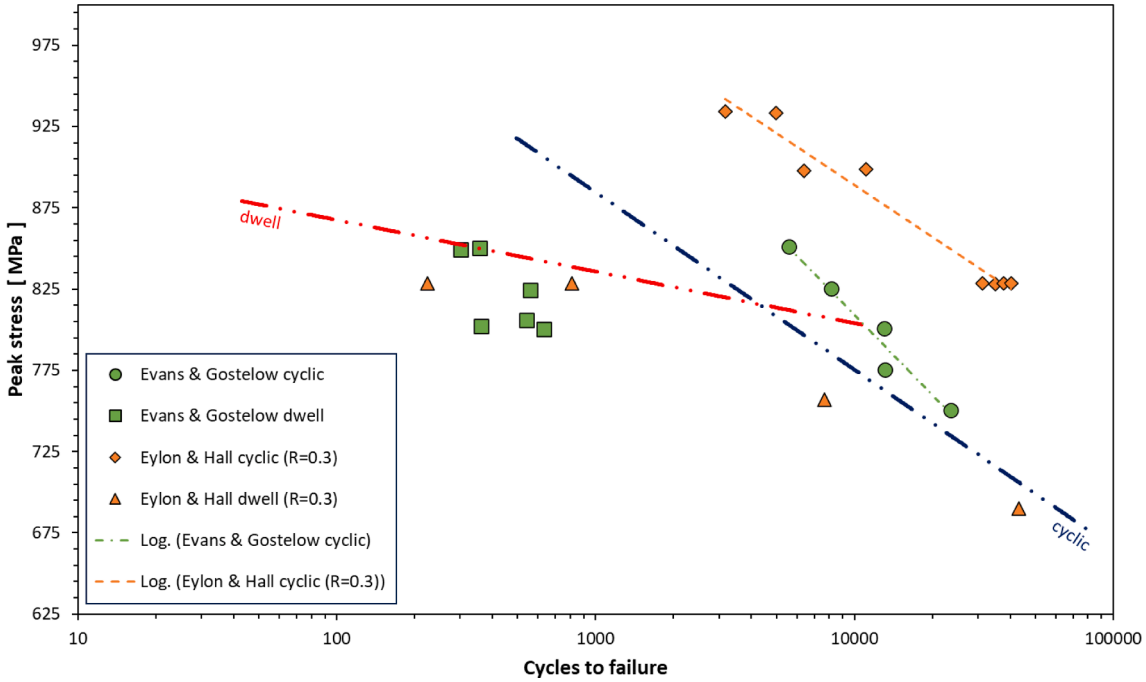

Fig. 17. Dwell sensitivity in varying forms of Ti-685 reported by different authors.

advent of EBSD, texture measurements were not available from either study, therefore precise details of the micro-texture in these materials are not reported. The source material for the present study, being hot rolled, small diameter, round bar stock, would have received greatest thermo-mechanical work. The recent EBSD measurements taken from our aligned specimens have indicated variations in α phase orientation from grain to grain but no obvious multi-grain MTRs were detected.

As an aside, the vacuum heat treatment applied to the bar stock employed by Evans and Gostelow [5] virtually reduced the internal hydrogen content of their alloy to zero (quoted at < 10 ppm). Despite this a significant dwell effect was noted. Given this information, together with the findings from subsequent studies where hydrogen contents were deliberately varied through vacuum heat treatment and re-charging [11,21], it is difficult to imagine how hydrides can be responsible for dwell behaviour.

So it is clear that the source of Ti-685 material can affect LCF performance in general and dwell sensitivity in particular. This also reads across to other titanium alloys. A similar effect was reported from this laboratory when characterising the fatigue behaviour of Ti 834. Hot rolled bar again failed to illustrate any apparent dwell debit in stark contrast to forged disc material [15]. Subsequent EBSD measurements illustrated greater texture and the presence of MTRs within the forged Ti

834 disc variant [19]. More recently, studies based on forgings with inhomogeneous microstructures have clearly identified dwell sensitivity in Ti 6Al 4 V [22,23] following a well-publicised service incident [24]. It must now be concluded that hot rolled bar stock materials are not appropriate for the prediction of dwell sensitivity in large scale forged components.

5. Conclusions

The following high level conclusions are drawn from the present research when considered in parallel with previous studies on Ti-685:

1. A definition for "engineering relevant dwell sensitivity" has been proposed, with fatigue lives $< 10^4$ cycles representing scientific interest only.
2. During the present investigation, utilising 6 mm diameter solid specimens, Ti-685 fatigue strength was sensitive to microstructure, with the basketweave variant displaying superior fatigue strength compared to aligned material. No engineering relevant dwell sensitivity was displayed by either the aligned or basketweave variants.
3. In contrast, previous testing conducted in this laboratory employing solid 9 mm diameter specimens has displayed a marginal dwell debit in this alloy at lives approximating 10^4 cycles. Specimen size or critically stressed volume in relation to microstructural features appears to affect LCF response.
4. Across the wider literature, Ti-685 has been shown to be dwell sensitive in fatigue regimes of interest to engineering components ($N_f > 10^4$), emphasising that the precise thermo-mechanical form under assessment is important when predicting dwell behaviour in engineering components.
5. In the context of "weak-strong" grain models to describe quasi-cleavage facet formation, colonies of α lath alignment can increase the local, coherent, slip band length and therefore the magnitudes of shear and tensile stress induced in the neighbouring strong grain.
6. Sub-surface fatigue crack initiation was widely detected in this alloy. This was not restricted to dwell loading scenarios or any specific microstructure.

CRediT authorship contribution statement

M.R. Bache: Conceptualization, Resources, Writing – original draft, Writing – review & editing. **J. Li:** Methodology, Investigation, Formal analysis, Visualization. **H.M. Davies:** Supervision, Writing – review & editing, Project administration.

Declaration of Competing Interest

The authors declare that they have no known competing financial interests or personal relationships that could have appeared to influence the work reported in this paper.

Data availability

Data will be made available on request.

Acknowledgements

All of the current mechanical tests were conducted at Swansea Materials Research & Testing Ltd. Recent technical discussions with Prof. Emeritus W.J. Evans are greatly appreciated.

References

[1] P. Pugh, *The Magic of a Name, The Rolls-Royce Story, Part 2: The Power Behind the Jets 1945 - 1987*, 2001, Icon Books UK/Totem Books USA.
[2] Harrison GF, Tranter PH, Evans WJ. Designing for dwell sensitive fatigue in near alpha titanium alloys. Proc Int Metal Conf Design Titanium, Bristol 1986.
[3] Wood WA. Formation of fatigue cracks. Philosoph Magaz 1958;3(31):692–9.
[4] Semiatin SL. An overview of the thermomechanical processing of α/β titanium alloys: Current status and future research opportunities. Metall Mater Trans A 2020;51:2593–625.
[5] Evans WJ, Gostelow CR. The effect of hold time on the fatigue properties of a β-processed titanium alloy. Metall Mater Trans A 1979;10A:1837–46.
[6] Eylon D, Hall JA. Fatigue behavior of beta processed titanium alloy IMI 685. Metall Trans A 1977;8(6):981–90.
[7] Bache M, Evans W. Tension and torsion fatigue testing of a near alpha titanium alloy. Int J Fatigue 1992;14(5):331–7.
[8] Evans WJ, Bache MR. The role of hydrogen in the fatigue response of a near alpha titanium alloy. In: Oikawa H, Maruyama K, Takeuchi S, Yamaguchi S, editors. Proc. 10th International Conference on Strength of Materials. Japan Institute of Metals; 1994. p. 493–6.
[9] Evans W, Bache M. Dwell-sensitive fatigue under biaxial loads in the near - alpha titanium alloy IMI685. Int J Fatigue 1994;16(7):443–52.
[10] Evans WJ, Bache MR. Fatigue under tension/torsion loading in IMI 685. In: Froes FH, Caplan I, editors. Seventh World Conference on Titanium. San Diego, California: TMMS; 1993. p. 1765–72.
[11] Evans WJ, Bache MR. The role of hydrogen in cyclic and dwell sensitive fatigue of a near alpha titanium alloy. In: Diego S, California FHF, Caplan I, editors. Seventh World Conference on Titanium. TMMS; 1993. p. 1693–700.
[12] Evans WJ. Optimising mechanical properties in alpha + beta titanium alloys. Mat Sci Eng 1998;243(1-2):89–96.
[13] Evans WJ. The influence of microstructure on dwell sensitive fatigue in a near alpha titanium alloy. Scripta Met 1987;21(4):469–74.
[14] Sinha V, Mills MJ, Williams JC. Understanding the contributions of normal-fatigue and static loading to the dwell fatigue in a near-alpha titanium alloy. Metall Mater Trans A 2004;35:3141–8.
[15] Bache MR, Cope M, Davies HM, Evans WJ, Harrison G. Dwell sensitive fatigue in a near alpha titanium alloy at ambient temperature. Int J Fatigue 1997;19(Supp. 1): S83–8.
[16] Bache MR. A review of dwell sensitive fatigue in titanium alloys: the role of microstructure, texture and operating conditions. Int J Fatigue 2003;25:1079–87.
[17] Stroh AN. The formation of cracks as a result of plastic flow. Proc Roy Soc (London) 1954;223:404–14.
[18] Bache M, Davies H, Davey W. Matthew Thomas and Iain Berment-Parr; "Microstructural control of fatigue behaviour in a novel α + β titanium alloy". Metals 2019;9:1200.
[19] Germain L, Bache MR. Crystallographic texture and the definition of effective structural unit size in titanium products. In: Ninomi M, Akiyama S, Ikeda M, Hagiwara M, Maruyama K, (eds.), Proc. 11th World Conf. on Titanium, Ti 2007 Science & Technology, The Japan Institute of Metals, pp. 953–956, 2007.
[20] Evans WJ. Private communication.
[21] Evans WJ, Bache MR. Hydrogen and fatigue behaviour in a near alpha titanium alloy. Scripta Met 1995;32:1019–24.
[22] Li J, Davies HM, Fox K, Mulyadi M, Glavicic MG, Bache MR. An appraisal of dwell sensitive fatigue in Ti-6Al-4V and the governing role of inhomogeneous microtexture. Int J Fatigue 2023;171:107589.
[23] Venkatesh V, Tamirisa S, Sartkulvanich J, Calvert K, Dempster I, Saraf V, Salem AA, Rokhlin S, Broderick T, Glavicic MG, Morton T, Shankar R, Pilchak A. ICME of microtexture evolution in dual phase titanium alloys. In: Hamish L. Fraser, M. Ashraf Imam, Yoji Kosaka, Henry J. Rack, Amit Chatterjee, and Andy Woodfield, TMS. Proc. of the 13th World Conference on Titanium, (The Minerals, Metals & Materials Society), pp. 1909-1912, 2016.
[24] BEA2017-0568, Investigation Report: Accident to the AIRBUS A380-861 equipped with Engine Alliance GP7270 engines registered F-HPJE operated by Air France on 30 September 2017 in cruise over Greenland (Denmark), in: Bureau d'Enquêtes et d'Analyses pour la sécurité de l'aviation civile. September 2020.